Hybrid integrated silicon nitride lasers

Jörn P. Epping[a], Arne Leinse[a], Ruud M. Oldenbeuving[a], Ilka Visscher[a], Douwe Geuzebroek[a], Dimitri Geskus[a], Albert van Rees[b], Klaus J. Boller[b], Michael Theurer[c], Martin Möhrle[c], Martin Schell[c], Chris. G.H. Roeloffzen[a], René G. Heideman[a]

[a]LioniX International B.V., Hengelosestraat 500, Enschede, The Netherlands 7521 AN;
[b]Univeristy of Twente, Drienerlolaan 5, Enschede, The Netherlands 7522 NB;
[c]Fraunhofer Heinrich-Hertz-Institute, Berlin, Germany, 10587;

ABSTRACT

Ultra-narrow linewidth tunable hybrid integrated lasers are built from a combination of indium phosphide (InP) and silicon nitride-based TriPleX™. By combining the active functionality of InP with the ultra-low loss properties of the TriPleX™ platform narrow linewidth lasers in the C-band are realized. The InP platform is used for light generation and the TriPleX™ platform is used to define a long cavity with a wavelength-selective tunable filter. The TriPleX™ platform has the ability to adapt mode profiles over the chip and is extremely suitable for mode matching to the other platforms for hybrid integration. The tunable filter is based on a Vernier of micro-ring resonators to allow for single-mode operation, tunable by thermo-optic or stress-induced tuning. This work will show the operational principle and benefits of the hybrid lasers and the state of the art developments in the realization of these lasers. High optical powers (>100 mW) are combined with narrow linewidth (< 1 kHz) spectral responses with tunability over a large (>100 nm) wavelength range and a low relative intensity (< -160 dB/Hz).

1. INTRODUCTION

Tunable semiconductor lasers with a narrow linewidth have found a wide range of applications, ranging from coherent optical communications [1], metrology [2,3], remote optical sensing such as LiDAR [4] and vibrometers [5] to arising applications such as microwave photonics [6,7]. While conventional semiconductor lasers such as distributed feedback (DFB) and distributed Bragg reflector (DBR) lasers are efficient in terms of footprint, cost-prize, and power consumption due to direct electrical pumping, their linewidths of around one MHz and tuning ranges of a few nanometers are limited due to high waveguiding losses in the semiconductor material and the resulting photon lifetime. To narrow the linewidths and further increase the tuning range external cavity diode lasers (ECDL) with a wavelength-selective element are used [8]. However, ECDLs that rely on high-cost bulk optical components and possibly mechanical movement lack robustness against harsh environments such as vibrations which is mandatory for bringing many of the aforementioned applications to the field.

Here, photonic integration can overcome those challenges. In particular, to achieve high-quality lasers with a narrow linewidth the combination of a low-loss passive and an active semiconductor material platform is needed. Here, the active semiconductor platform offers the optical gain while the passive platform offers low propagation losses to increase the photon lifetime and allow for tunable narrowband wavelength filters. To combine two complementary material platforms, the two main approaches are heterogenous and hybrid integration. The former refers to integrations of two material platforms by wafer bonding during fabrication, while the latter refers to assembling two photonic integrated circuits after dedicated chip fabrications. At first glance, to achieve cost-effective wafer-scale production obviously heterogenous integration is most favourable, but it has been recently shown that hybrid integration by flip-chipping can give similar results and also enables hybrid integration on a wafer-scale [9]. This new approach is described in Section 3.3.

However, so far most hybrid as well as heterogeneously integrated lasers often lack sufficient optical power for applications in optical communications and microwave photonics. Especially, since for efficient heterogenous integration high refractive index materials such as silicon have to be used [10]. The use of silicon-based waveguide ultimately limits the achievable output power due to its damage threshold as well as the wavelength range. However, silicon nitride-based waveguides can support high optical powers due to their high damage threshold in the C-band.

Recently, we developed a hybrid integrated photonic platform [11] based on active InP components such as gain sections, modulators, and detectors with passive silicon nitride-based TriPleX™ offering low propagation losses of < 0.1 dB/cm. The low propagation losses enable a high photon lifetime resulting in a low intrinsic linewidth of hybrid integrated lasers as well as high optical output powers due its high damage threshold. In this work, we present the latest results of our hybrid integrated lasers comprising of an InP semiconductor optical amplifier and a wavelength-selective TriPleX™ mirror.

2. LASER DESIGN

The laser design for hybrid integrated lasers has been extensively reported [12-15]. In this section a brief summary of the basic design rules and ideas is provided. First of all, to ensure that the laser has a narrow linewidth (< 1 kHz), a large tuning range (> 100 nm) as well as a high optical output power (> 100 mW) the coupling losses between the separate integrated optical platforms, InP and TriPleX™, as well as fiber-chip coupling losses have to be minimal. Both coupling losses can be minimized by matching the mode field diameter (MFD) at the facet of the TriPleX™ waveguide via tapering. By tapering and engineering the TriPleX™ double-stripe geometry in height as well as width [11], a single TriPleX™ chip can be designed to match its MFD at the coupling region to an InP waveguide on the one side and that of a single mode fiber (SMF) on the other side. By mode engineering losses of ≈1 dB per facet between InP and TriPleX™ and 0.5 dB per facet between SMF and TriPleX™ have been achieved. The so-called asymmetric double-strip geometry [11], as used predominately in this work, exhibits low propagation losses of less than 0.1 dB/cm over the full C-band, while offering bend radii of down to 80 µm without any significant radiation losses.

To control the wavelength of the hybrid integrated laser a set of wavelength-selective components is combined. In our case, two ring resonators in a specific configuration effectively form a wavelength-selective mirror. A single ring resonator has a certain free spectral range (FSR) and its resonant wavelength can be thermally tuned. When the mirror only contains a single ring, this means the laser can be tuned only over this range. So the tuning range of the laser depends on the physical roundtrip length of the ring. Actually, due to fabrication tolerances the resonator of choice is a race-track type over a micro-ring resonator as it provides better control of the coupling coefficient. Keeping in mind the minimum bend radius, the smallest ring that can be fabricated has a roundtrip length of about 850 µm, which corresponds to an FSR of about 1.6 nm around a wavelength of 1550 nm. The schematic of a ring resonator mirror with a single ring and the corresponding spectral response is shown in Figure 1.

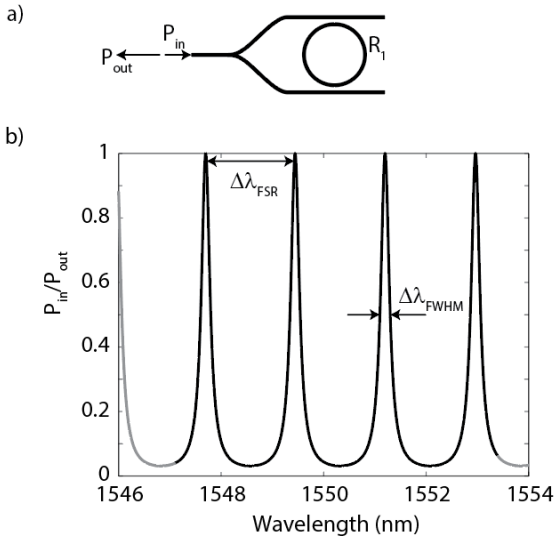

Figure 1. Schematic layout of a ring resonator mirror with a single ring resonator with radius R_1. (b) Reflected power vs. input wavelength calculated for a ring resonator with an FSR of about 1.6 nm.

The FSR of a single ring resonator can be calculated by

$$\Delta\lambda_{FSR} = \frac{\lambda_0^2}{n_g L} \tag{1}$$

With center wavelength λ_0 = 1550 nm, group index of the waveguide n_g =1.77 and the ring circumference, L.

The spectral width of the resonant peaks can be calculated by

$$\Delta\lambda_{FWHM} = \frac{\lambda_0^2}{\pi n_g L} \cdot \frac{\kappa^2}{\sqrt{1-\kappa^2}} \tag{2}$$

In this expression, κ is a coefficient which describes the coupling of the electric field amplitude from the input waveguide to the ring resonator.

To ensure a tuning over the entire telecommunication C-band, this tuning range needs to be increased. This can be done by adding a second ring with slightly different circumference in series to the first ring, exploiting the Vernier principle to increase the total FSR of the ring, $\Delta\lambda_{FSR,tot}$. An example of the spectral response of such a double-ring mirror is shown in Figure 2. For this example, we have chosen the described FSR of 1.6 nm for the first ring while the second ring has a 10% larger radius.

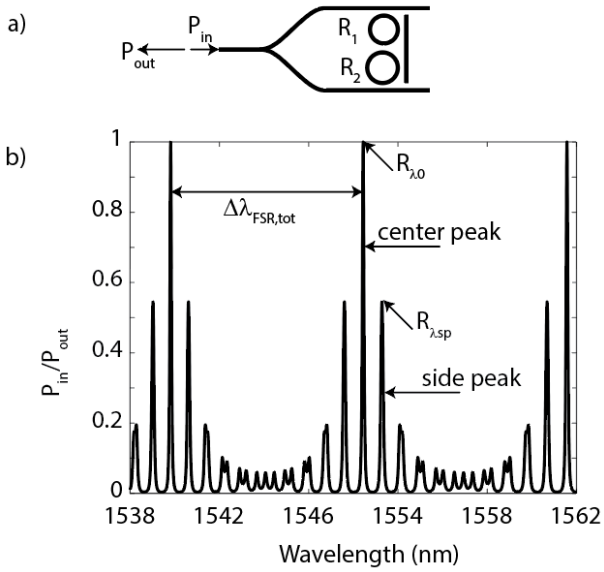

Figure 2. a) Schematic layout of a ring resonator mirror with two differently sized rings with R_1 and R_2 radii. b) Reflected power vs. input wavelength calculated for a ring resonator with an FSR of about 1.6 nm, while the second ring has a 10% larger radius.

To build the hybrid integrated laser, the reflective filter is combined with an RSOA to provide the optical gain. To ensure that the tuning range is indeed $\Delta\lambda_{FSR,tot}$, the light that is reflected at the center peak, $R_{\lambda 0}$, needs to have a larger gain, $G_{\lambda 0}$, than the light at the side peak, $R_{\lambda sp}$. Otherwise, the tuning range would still be limited to the FSR of a single ring. The amount of light that is reflected at $R_{\lambda sp}$ depends on the Q-factors of the both rings; a higher Q value will result in a lower $R_{\lambda sp}$. In other words, depending on the roundtrip length of the ring, the coupling coefficient κ and the propagation loss of the waveguide, the side peak can be decreased enough to fulfill the design condition $R_{\lambda sp} * G_{\lambda sp} < R_{\lambda 0} * G_{\lambda 0}$.
The schematic of a typical hybrid integrated laser is shown in Figure 3. The laser comprises of an InP reflective semiconductor optical amplifier (RSOA) and wavelength-selective micro-ring mirror in TriPleX™. The InP has a high reflectivity (HR) coating on one side and an anti-reflection (AR) coating matching the refractive index of the TriPleX™ chip.

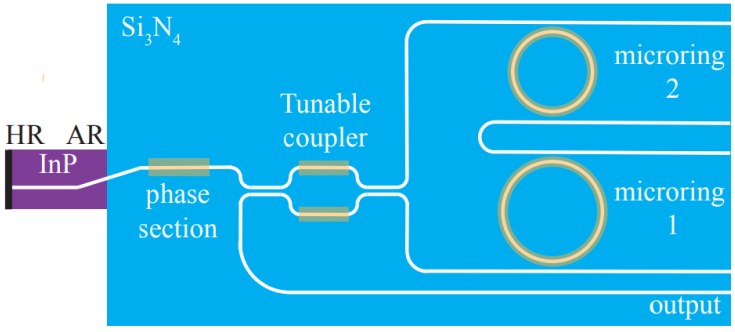

Figure 3. Schematic of a hybrid integrated laser with an InP RSOA (purple) and a TriPleX™ (blue) ring resonators mirror with a tunable output coupler. Thermo-optic tuners are indicated in orange[17].

3. LASER PACKAGING

3.1. Device Assembly

For efficient hybrid integration of the InP gain section has to be actively aligned to the TriPleX™ chip. Firstly, the fiber array is attached to the TriPleX™ chip. Secondly, to a feedback signal for alignment the gain section is electrically powered and the emitted optical power is measured using the optical fiber. Fixation of the individual components is carried out using an epoxy. Finally, the module can be placed inside a butterfly housing with a build-in Peltier element. An example of such an hybrid integrated laser assembly is shown in Figure 4.

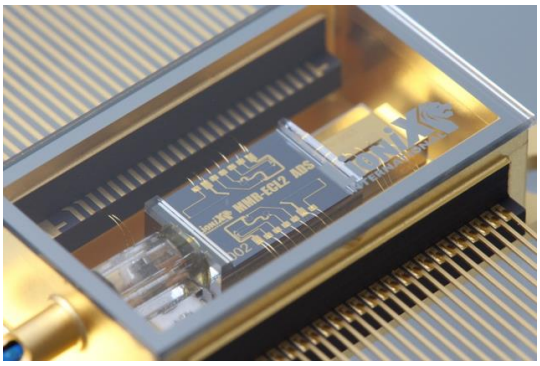

Figure 4. Photograph of a hybrid integrated laser in a butterfly package.

3.2. Vibration Tests

For airborne applications, the optical assemblies have to withstand severe environmental conditions which can result in, e.g., temperature changes and vibrations. To test the mechanical robustness of the laser modules vibration tests were performed at the Netherlands aerospace center (NLR). The vibration tests were according to the test standards defined by the Radio Technical Commission for Aeronautics (RTCA) and have to demonstrate that the assemblies are in compliance with standards for airborne equipment. During the test we applied a reference vibration spectrum of the random vibrations according to the test standard RTCA DO-160G. Two photographs of the test setup are shown in Figure 5. In this test the laser modules had to pass the RMS-value of the overall spectrum of 4.12 g_{rms} with an applied probability of 3σ. This spectrum was imposed on 3 integrated hybrid laser modules as shown Figure 5 for a duration of 60 minutes. Each laser module was mounted in X, Y and Z directions such that during the test run all directions were tested.

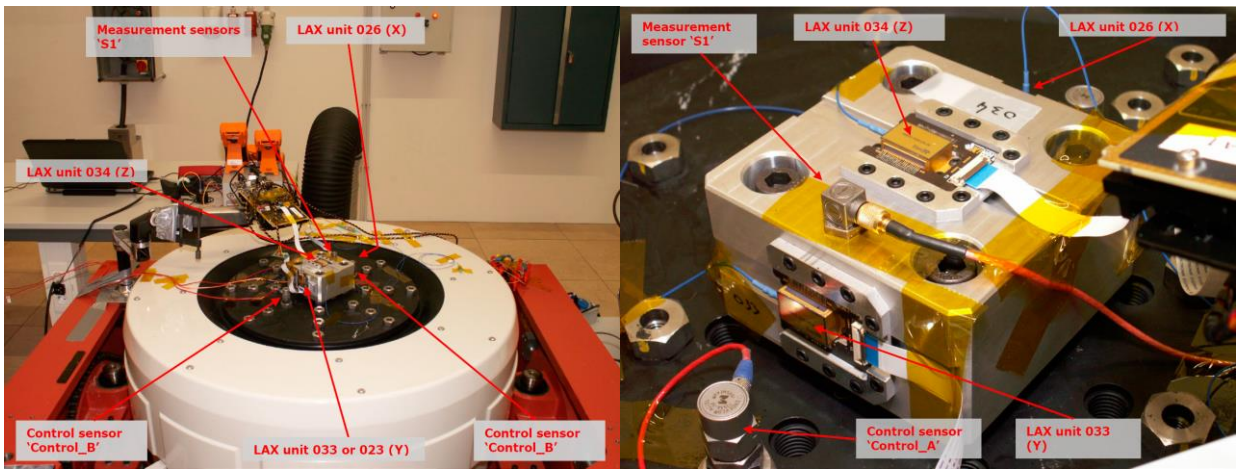

Figure 5. Photographs of the vibration test setup (left) and vibrational mount for 3 hybrid integrated lasers (right).

After reaching the target level of 4.12 g_{rms}, the tests were continued to determine the design margin in terms of vibrations. The test level reached the maximum available level of 40.9 g_{rms}, having a 3σ value of 123 g, which was solely limited by the vibrational test setup. For a video of the testing at the highest available level see Video 1. However, during the vibration tests not a single failure was detected, while all 3 laser modules were continuously running and their optical output power was monitored. The positive outcome of the vibrational tests shows the intrinsic robustness of integrated photonic modules by hybrid integration which is mandatory for applications in automotive, aircraft, and space.

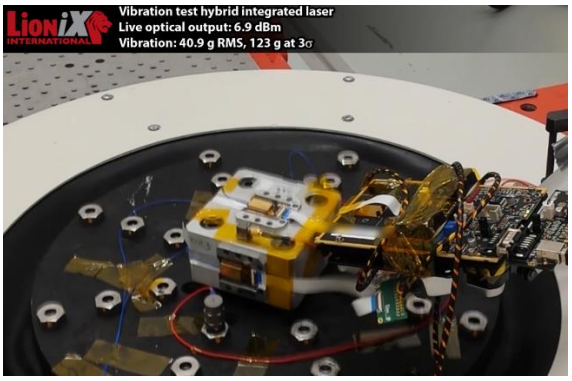

Video 1. Vibration test of the integrated hybrid lasers. http://dx.doi.org/doi.number.goes.here

3.3. Flip-Chip Integration

As an advanced hybrid integration scheme, we developed an interface dedicated for flip-chip integration of InP on TriPleX™ as shown in Figure 6. In our new approach, the InP chip integration is not limited to the TriPleX™ chip edges and can thus be applied with TriPleX™ on a wafer scale, which makes it a preferred solution for high volume production. As shown in Figure 6 (right) the InP chip is mounted p side down into an etched recess on the TriPleX™ chip or wafer. The silicon oxide layer of the TriPleX™ chip is etched through to the silicon substrate for optimum heat dissipation. Precise mechanical alignment stops are implemented for passive vertical alignment of the optical modes. Special visual alignment marks with high accuracy relative to the optical mode are implemented on the InP and TriPleX™ chips for horizontal alignment.

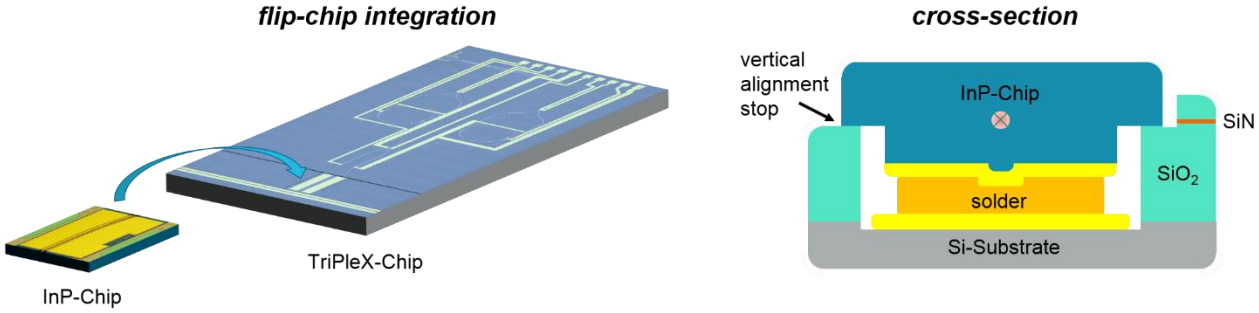

Figure 6. Flip-chip integration of InP chip into etched recess on TriPleX™ chip (left) and cross-section through InP chip bonded to TriPleX™ chip (right).

Additionally, the integration interface is suitable for active alignment as shown in [9, 16]. The InP and TriPleX™ chips both comprise spot-size converters for mode matching and increased alignment tolerance. To mitigate residual reflection from the chip-to-chip interface the waveguide on each side is tilted and the air gap is filled with an UV-curable glue to match the effective refractive index of TriPleX™. The front facet of the InP chip is coated with an antireflection (AR) coating. The integration interface is suitable for consecutive integration of multiple InP chips on the same TriPleX™ chip or wafer as demonstrated in Figure 7 (left). Thanks to the passive vertical alignment even full InP arrays can be integrated with no added complexity as to single chip integration (see Figure 7 (right)). To demonstrate the feasibility of the flip-chip interface InP DFB lasers have been integrated on a TriPleX™ chip. Using our new approach we achieved a chip-to-chip coupling loss of -1.6 dB only and an optical power coupled to the silicon nitride waveguide exceeding 60mW [16]. This

result is comparable to conventional active alignment and enables hybrid integration on a wafer-scale between InP and TriPleX™.

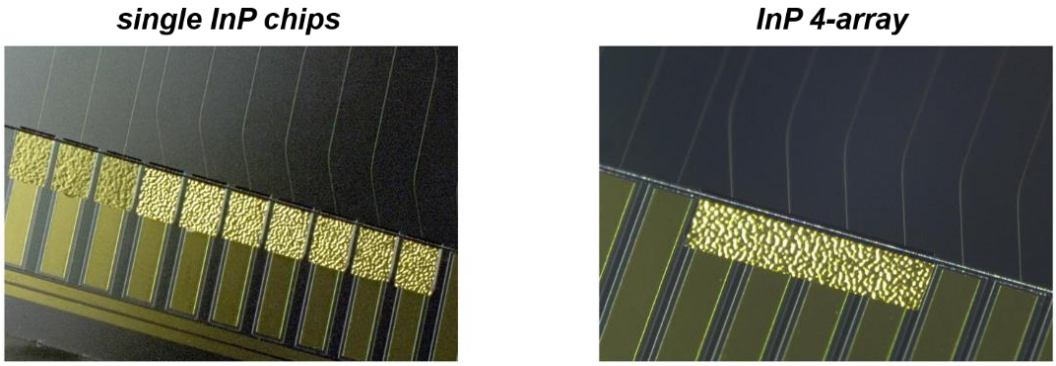

Figure 7. Photograph of multiple InP chips (left) and InP 4-array (right) flip-chip integrated onto TriPleX™ chip.

4. LASER CHARACTERISTICS

In section, the typical laser characteristics are presented. To control the output coupling of the laser cavity a tunable coupler is used and a in standard laser design an output coupling around 80% results in the highest output power. At a pump current of 300 mA output powers of 17 dBm (50 mW) in the C-band (1530-1560 nm) at single-mode operation have been achieved at the fiber output.

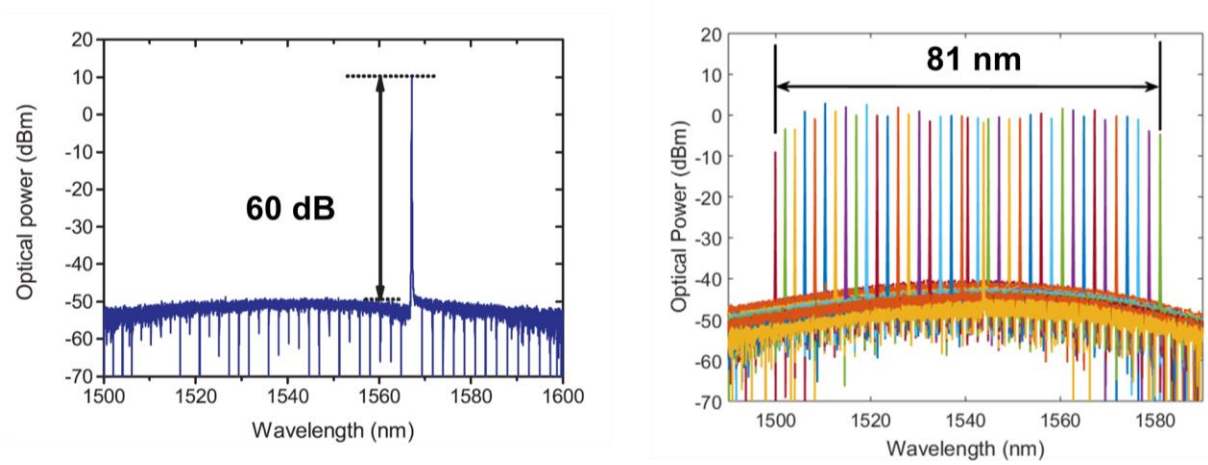

Figure 8. Optical spectrum of a hybrid integrated laser module in single mode operation with an optical signal to noise ratio of 60 dB (left). Superimposed optical spectra covering a total of more than 80 nm tuning range (right). Increased tuning ranges of 120 nm have been reported [17].

To ensure that the optical output power is indeed in a single mode an optical signal to noise ratio (OSNR) is important. Figure 8 (left) shows the optical spectrum of our hybrid integrated laser and an OSNR of 60 dB can been seen confirming that almost all light is emitted at one wavelength and no side-modes are visible. To set the wavelength of the hybrid integrated laser the micro-ring resonators on the TriPleX™ chip can be controlled with thermo-optic tuners. To demonstrate the tunability of the hybrid integrated laser we measured a set of spectra over the whole tuning range of the hybrid integrated laser. The obtained superimposed optical spectra are shown in Figure 8 (right) and are showing a total tuning range of 81 nm. It can be seen that the optical power drops at the edges of the gain spectrum. But also increased tuning ranges of up to 120 nm have been reported using our hybrid integrated laser [17]. Note, that this wavelength tuning is discrete and that the mode-hop-free tuning range is far smaller. Typically our hybrid integrated laser can be tuned a few 10s of picometers before a mode-hop occurs, however, it has recently been shown that the mode-hop-free tuning range can be increased by simultaneously tuning the phase section (see Figure 3) of the laser and a mode-hop-tuning range of 0.22 nm has been reported [18].

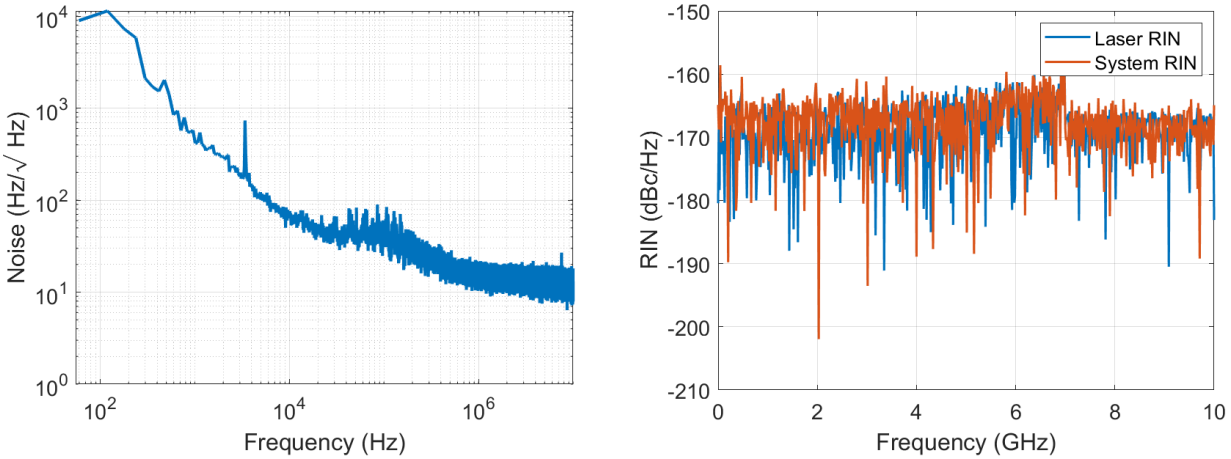

Figure 9. Frequency noise spectrum (left) and relative intensity noise (RIN, right) of a hybrid integrated laser. The frequency noise spectrum shows an intrinsic linewidth of less than 800 Hz (left).

For many application the noise characteristics of the laser modules are critical. Here, we measured both the frequency noise and the relative intensity noise (RIN) spectrum of our hybrid integrated laser. While the frequency noise power spectral density (PSD) spectrum is e.g. linked to the intrinsic linewidth of the laser, a low RIN is important to have a sufficient signal-to-noise ratio. In Figure 9 example measurements of both the frequency noise and the RIN spectrum are shown. Due to the low propagation losses in TriPleX™ a long photon lifetime can be realized in the cavity resulting in a low intrinsic linewidth. In Figure 9 (left) the frequency noise spectrum is shown. The frequency noise was measured using linewidth analyzer (HighFinesse LWA-1k) and shows a white noise floor at 15 Hz/Hz$^{1/2}$ which corresponds to an intrinsic linewidth of less than 800 Hz. As to date, the lowest intrinsic linewidth in a hybrid integrated laser that has been reported is as low as 40 Hz by using a micro-ring mirror with 3 rings resonators [19]. We measured the relative intensity noise (RIN) of the hybrid integrated laser using a high-speed detector and an electrical spectrum analyzer up to a frequency of 10 GHz. The RIN measurement is shown in Figure 9 (right) and it can be seen that the RIN (shown in blue) is well below -160 dBc/Hz over the whole measurement range and for most of the frequencies even as low as -170 dBc/Hz. This RIN measurement is in correspondence with the calculated RIN of -165 dBc/Hz based on the optical spectrum analyzer measured OSNR of 60 dB. Additionally, we show the relative system noise (RIN and shot noise) shown in red as a comparison to the RIN.

3.4. Dual Gain Laser

As many applications such as, e.g., microwave photonics and optical ranging improve with higher optical powers, we changed the cavity design of the hybrid integrated laser to increase its output power. By changing the TriPleX™ chip design two InP RSOAs can be coupled to a single TriPleX™ chip. The scheme and a photograph of the dual-gain section hybrid integrated laser is shown in Figure 10 a) and b), respectively. Here, the hybrid integrated laser comprises of two InP RSOAs chips and a low-loss TriPleX™ wavelength-selective filter chip. The wavelength-selective filter is similar to the one shown in Figure 7. However, to achieve a higher optical output power the filter chip is coupled to two individual InP RSOAs with a length of 700 µm instead of one [12,13,19]. The coupling losses from the InP RSOAs to TriPleX™ laser cavity are estimated to be about 1 dB. Each of the RSOAs has an individual electrical connection to apply a pump current. On the TriPleX™ chip, thermo-optic tuners are used to set the wavelength-selective filter and to control the phase of the cavity. To combine both the laser output coupling of the cavity and the power in the output waveguide two tunable Mach-Zehnder couplers are used. The output waveguides are coupled to a fiber array with standard polarization maintaining fibers with a coupling loss of 0.5 dB.

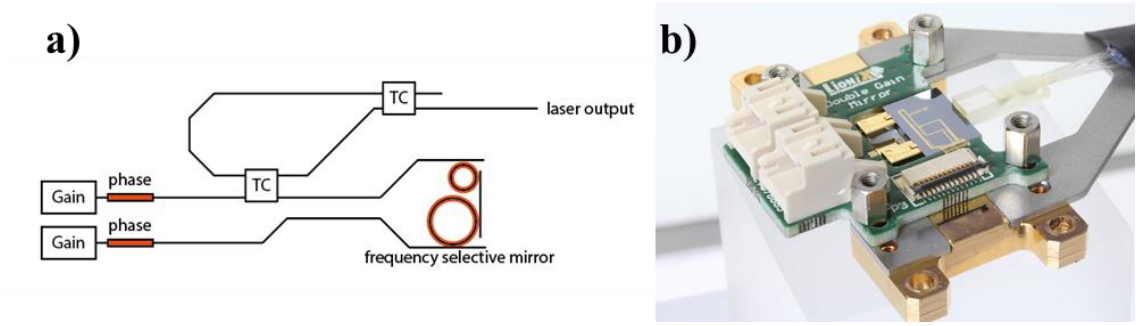

Figure 10. a) Conceptual design of the dual gain laser cavity consisting of a tunable dual-ring cavity, two gain section with phase tuners, and two tunable Mach-Zehnder couplers (TC) to control the output coupling and output power. b) Photograph of the assembled dual gain laser.

Using this novel design, we achieved a record maximum output power of 20.2 dBm at the fiber output and an on-chip power of 20.7 dBm at a pump current of 300 mA at both RSOAs. The fiber-output power as a function of pump current at each gain section is shown in Figure 11 a) and it can be seen that at pump currents above 300 mA the RSOAs saturate due to insufficient cooling. Note that the output power by using two RSOAs is indeed twice as much when compared to devices with only one RSOA and a similar cavity design, where the maximum obtained optical output power is about 17 dBm. The resulting output power is, to the best of our knowledge, the highest power achieved with any hybrid integrated laser to date. Furthermore, we tuned the frequency selective filter and measured the achieved output power as a function of wavelength. The results are shown in in Figure 11 b) and it can be seen that the wavelength of the laser can be tuned over 100 nm at a -1 dB power drop and a total range of 119 nm from 1468 nm to 1587 nm. Over the whole tuning range, the laser operated at a single mode with an OSNR of more than 60 dB.

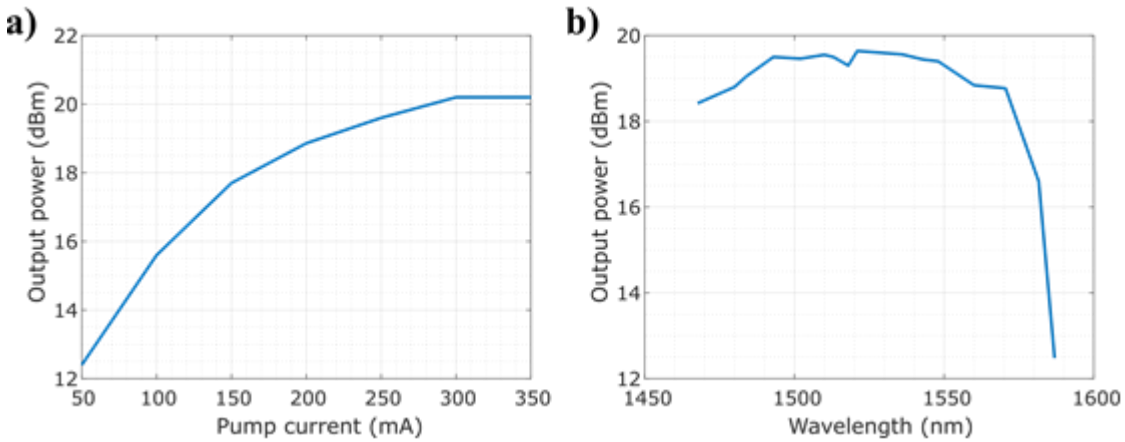

Figure 11. a) Fiber-output power as a function of pump current at each gain section. Gain saturation is reached at pump currents of 300 mA. b) Fiber-output power as a function of laser wavelengths. At a -1 dB drop in output power a tuning range of 100 nm is reached.

Similar to the single-gain hybrid integrated laser we measured the frequency noise of the dual-gain laser and its RIN as shown in Figure 12 a) and b), respectively. Note that during the frequency noise measurements the thermo-optic tuners of the dual-gain laser were inactive due to electric noise induced by the heater drivers, while both gain sections were driven with a pump current of 100 mA. It can be seen that the white noise floor reaches a level of 10 $Hz/Hz^{1/2}$ corresponding to an intrinsic linewidth of the laser of around 320 Hz, which is comparable low to intrinsic linewidths in single-gain hybrid integrated lasers with a similar resonator design. The RIN measurement is shown in Figure 12 b) and it can be seen that the RIN (shown in blue) is well below -160 dBc/Hz over the whole measurement range and for most of the frequencies at a level as low as -170 dBc/Hz. Additionally, we show the relative system noise shown in red as a comparison to the RIN. Due to its increased output power of more than 20 dBm and similar noise characteristics compared to the single-gain laser, the dual gain laser meets the requirements many applications.

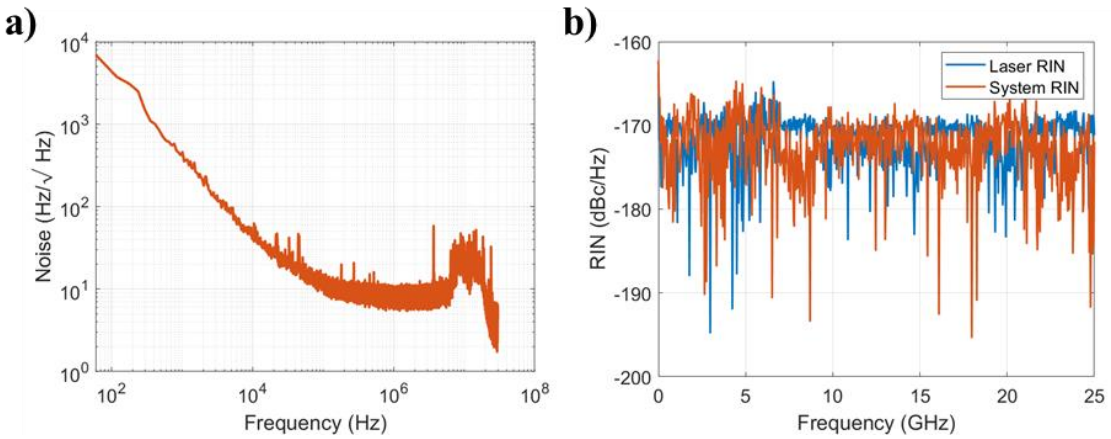

Figure 12. Frequency noise measurement of the dual-gain laser showing an intrinsic linewidth of 300 Hz. b) Measured relative intensity noise (RIN) of the laser and the system for frequencies up to 25 GHz.

5. CONCLUSION AND OUTLOOK

In conclusion, we presented that excellent hybrid integrated lasers with sub-kHz intrinsic linewidths and output powers of more than 20 dBm were realized by combining the two complementary integrated photonic platforms, active InP and low-loss silicon nitride-based TriPleX™. Furthermore, their broad tuning range of almost 120 nm and low relative intensity noise of less than -160 dBc/Hz make them excellent light sources for many applications. Due to their intrinsic stability hybrid integrated lasers can also withstand harsh environmental conditional as was demonstrated by extreme vibration tests. To achieve low-cost production of hybrid integration it has been shown that flip-chip integration on a wafer scale can be applied using these platforms. The functionality of the hybrid integrated laser can be further extended by adding modulators and photo-detectors in a single assembly.

So far, all presented hybrid integrated lasers worked at wavelength around 1550 nm. The range of wavelengths can be extended, especially into the near infrared and visible wavelength ranges, by making use versatility of TriPleX™ with its broad transparency range (400 nm - 2300 nm) and adaptable mode field by the choice of gain material. The first hybrid integrated laser at visible wavelength of 680nm has just been realized in TriPleX™ [20].

ACKNOWLEDGEMENTS

This project has received funding from the European Union's Horizon 2020 research and innovation program under grant agreement 762055 (BlueSpace) and 780502 (3PEAT).

The authors would like to acknowledge the collaboration with partner Viasat. This work was funded under ESA contract reference No. 40000121956/17/NL/CLP.

REFERENCES

[1] Zhang, S., Kam, P. Y., Yu, C., and Chen, J., "Laser linewidth tolerance of decision-aided maximum likelihood phase estimation in coherent optical M-ary PSK and QAM systems," IEEE Photonics Technol. Lett. 21, 1075–1077 (2009).

[2] Lezius, M., Wilken, T., Deutsch, C., Giunta, M., Mandel, O., Thaller, A., Schkolnik, V., Schiemangk, M., Dinkelaker, A., Kohfeldt, A., et al., "Space-borne frequency comb metrology ," Optica 3, 1381–1387 (2016).

[3] Newman, Z.L., Maurice, V., Drake, T., Stone, J.R., Briles, T.C., Spencer, D.T., Fredrick, C., Li, Q.,Westly, D., Ilic, B.R., et al., "Architecture for the photonic integration of an optical atomic clock," Optica 6, 680–685 (2019).

[4] Hecht, J., "Lidar for Self-Driving Cars," Opt. Photonics News 29, 26–33 (2018).

[5] Li, Y, Segers, P., Dirckx, J., and Baets, R., "On-chip laser Doppler vibrometer for arterial pulse wave velocity measurement," Biomed. Opt. Express 4(7), 1229-1235 (2013).

[6] Marpaung, D., Yao, J., and Capmany, J., "Integrated microwave photonics," Nat. Photonics 13, 80–90 (2019).

[7] Marpaung, D., Roeloffzen, C.G.H., Heideman, R.G., Leinse, A., Sales, S., and Capmany, J., "Integrated microwave photonics," Laser Photonics Rev. 7(4), 506–538 (2013).
[8] Harvey, K.C., and Myatt, C.J., "External-cavity diode laser using a grazing-incidence diffraction grating," Opt. Lett. 16(12), 910-912 (1991).
[9] Theurer, M., et al., "Flip-Chip Integration of InP and SiN," IEEE Photonics Technol. Lett. 31(3), 273–276 (2019).
[10] Xiang, C., Jin, W., Guo, J., Peters, J.D., Kennedy, M.J., Selvidge, J., Morton, P.A., Bowers, J.E., "Narrow-linewidth III-V/Si/Si3N4 laser using multilayer heterogeneous integration," Optica 7(1), 20-21 (2020).
[11] Roeloffzen, C.G.H., et al., "Low-loss Si_3N_4 TriPleX™ optical waveguides: Technology and applications overview," IEEE J. Sel. Top. Quantum Electron 24 (4), 1-21 (2018).
[12] Oldenbeuving, R.M., Klein, E.J., Offerhaus, H.L., Lee, C.J., Song, H., Boller, K.J. ,"25 kHz narrow spectral bandwidth of a wavelength tunable diode laser with a short waveguide-based external cavity," Laser physics letters 10 (1), 015804 (2013).
[13] Fan, Y., Epping, J.P., Oldenbeuving, R.M., Roeloffzen, C.G.H., Hoekman, M., Dekker, R., Boller, K.J., "Optically Integrated InP–Si_3N_4 Hybrid Laser," IEEE Photonics J. 8(6), 1-11. (2016).
[14] Oldenbeuving, R.M., "Spectral control of diode lasers using external waveguide circuits," PhD. Thesis, University of Twente (2013).
[15] Tran, M.A., Huang, D. , Bowers, J.E., "Tutorial on narrow linewidth tunable semiconductor lasers using Si/III-V heterogeneous integration," APL Photonics **4**, 111101 (2019).
[16] Theurer, M., et al., "Actively Aligned Flip-Chip Integration of InP to SiN Utilizing Optical Backscatter Reflectometry," Proc. ECOC, Dublin, Ireland, 1–4 (2019).
[17] Boller, K.J., et al., "Hybrid Integrated Semiconductor Lasers with Silicon Nitride Feedback Circuits," Photonics 7(1), 4 (2020).
[18] van Rees, A., Fan, Y., Geskus, D., Klein, E.J., Oldenbeuving, R.M., van der Slot, P.J.M., Boller, K.J., "Ring resonator enhanced mode-hop-free wavelength tuning of an integrated extended-cavity laser," arXiv:1912.09455 (2019).
[19] Fan, Y., van Rees, A., van der Slot, P.J.M., Mak, J., Oldenbeuving, R.M., Hoekman, M., Geskus, D,. Roeloffzen, C.G.H., Boller, K.J., "Ultra-narrow linewidth hybrid integrated semiconductor laser," arXiv:1910.08141 (2019).
[20] Franken, K., van Rees, A., Fan, Y., Geskus, D., Dekker, R., Geuzebroek, D., Fallnich, C., van der Slot, P.J.M., Boller, K.J., "First realization of a hybrid integrated diode laser in the visible spectral range," SPIE OPTO, San Francisco, United States, 11301-71 (2020).